Available online at www.sciencedirect.com

ScienceDirect

Ceramics International 39 (2013) 9613–9617

CERAMICS INTERNATIONAL

www.elsevier.com/locate/ceramint

Combustion synthesis and spectroscopic charaterisation of $LaAlO_3$ nanophosphors doped Er^{3+} ions ☆

A. Dhahri[a], K. Horchani-Naifer[a,*], A. Benedetti[b], F. Enrichi[c], M. Ferid[a]

[a] *Laboratoire de Physico-chimie des Matériaux Minéraux et leurs Applications, Centre National des Recherches en Sciences des Matériaux, Technopole de Borj Cedria, B.P. 73, 8027 Soliman, Tunisia*

[b] *Dipartimento di Scienze Molecolari e Nanosistemi, Università Ca' Foscari Venezia, Dorsoduro 2137, 30123 Venezia, Italy*

[c] *CIVEN (Coordinamento Interuniversitario Veneto per le Nanotecnologie), via delle Industrie 5, 30175 Marghera, Venezia, Italy*

Received 10 February 2013; received in revised form 6 May 2013; accepted 20 May 2013
Available online 2 June 2013

Abstract

Lanthanum aluminate ($LaAlO_3$) nanophosphors doped with erbium were successfully synthesized by a combustion process. The powders were characterized X-ray diffraction (XRD), scanning electron microscopy (SEM), transmission electron microscopy (TEM) and fluorescence spectroscopy. Pure $LaAlO_3$ phase was obtained at 800 °C heated for 4 h, with an average crystal size, as determined by TEM, of 60 nm. Infrared emission spectra and decay times of main luminescence transitions were measured at room temperature. A strong emission is reported at 1550 nm from the ($^4I_{13/2} \rightarrow {}^4I_{15/2}$) transition, which intensity depends on the Er concentration.

Keywords: Combustion process; Lanthanum aluminate; Erbium; Nanoparticule; Photoluminescence

1. Introduction

Lanthanum aluminate ($LaAlO_3$) with a perovskite-type structure has at room temperature a rhombohedral structure with R-3c symmetry and it undergoes phase transition into the Pm-3 m cubic phase at $T_c = 527$ °C [1]. Typically, $LaAlO_3$ has been prepared by conventional solid-state reaction of Al_2O_3 and La_2O_3 in the temperature range of 1500–1700 °C [2,3]. But this method suffers from many inherent shortcomings, such as the high-temperature heat treatment which has a detrimental effect on the grain size.

Recently $LaAlO_3$ has been successfully prepared by a novel two-step process [4] and microwave irradiation [5]. Moreover, various wet and soft chemical methods including the polymerized complex method using citric acid and ethylene glycol route have been reported [6]. Several low temperature (750–900 °C) chemical routes are used for preparing finer and homogeneous powders of $LaAlO_3$ like polyvinyl alcohol (PVA) with metal nitrate synthesis [7], sol–gel process [8–10], EDTA gel route [11,12], co-precipitation method [13,14], pyrolysis using triethanolamine [15] and combustion synthesis with urea and hydrazine as fuel [16–19].

This paper presents the synthesis and characterization of $LaAlO_3{:}Er^{3+}$ phosphors prepared by combustion synthesis [20,21], which has the advantage of being simple, fast and economical in doping. The structural details and the optical properties of the synthesized phosphors have been investigated by X-ray diffraction (XRD), transmission electron microscopy (TEM), scanning electron microscopy (SEM), and fluorescence spectroscopy. The photoluminescence emission and excitation as well as the decay times were measured.

2. Experimental procedure

The starting materials were lanthanum nitrate hexahydrate $[La(NO_3)_3 \cdot 6H_2O]$ (98%), aluminum nitrate nonahydrate $[Al(NO_3)_3 \cdot 9H_2O]$ (99%), erbium(III) nitrate pentahydrate $[Er(NO_3)_3 \cdot 5H_2O]$, and glycine $[H_2NCH_2COOH]$ (99%).

☆**Foundation item:** Project supported by the Ministry of Higher Education, Scientific Research and Technology of Tunisia.

*Corresponding author.
E-mail address: karima_horchani@yahoo.com (K. Horchani-Naifer).

0272-8842/$ - see front matter © 2013 Elsevier Ltd and Techna Group S.r.l. All rights reserved.
http://dx.doi.org/10.1016/j.ceramint.2013.05.082

$La(NO_3)_3 \cdot 6H_2O$ and $Al(NO_3)_3 \cdot 9H_2O$ $Er(NO_3)_3 \cdot 5H_2O$ and H_2NCH_2COOH were dissolved in distilled water. Er^{3+} ions doped lanthanum aluminate with general formula $(La_{1-x}Er_x)AlO_3$ were prepared with different concentrations of Er (x=2%, 5%, 10%). During the process, the molar ratio of glycine to total metal cations concentration G/M was 2 and the cation ratio of La:Al was 1:1. Glycine was used as a fuel. The resulting solution was magnetically stirred at 85 °C to get a clear and uniform solution. The solution slowly turned viscous on continued heating for about 1.5 h, becoming a highly viscous gel. Throughout the process, no signs of precipitation or turbidity were observed. The gel was put into a vacuum oven and kept at 110 °C for 24 h, undergoing rapid dehydration and foaming followed by decomposition and generating a solid precursor. Finally this solid precursor was ground to fine powders and was calcined at different temperatures (600 °C, 700 °C and 800 °C) for 4 h to obtain pure $LaAlO_3$.

3. Experimental

The X-ray powder diffraction (XRD) patterns of all the samples were recorded on a Philips X'Pert system (PW3020 vertical goniometer and PW3710 MPD control unit) with CuKα1,2 radiation (λ_1=1.54059 Å and λ_2=1.54442 A°). In order to improve the signal to noise ratio, at least three runs (collected with 10 s/step and 0.05 °/step) were measured.

The scanning electron images of samples were recorded with scanning electron microscope (SEM) JEOL JSM-5600LV, operated at 20 kV equipped with an Oxford Instruments ISIS series 300 EDS detector.

The morphology of products was characterized by transmission electronic microscopy (TEM) (Tecnai G2 ultra Twin). TEM images were taken at 300 kV with a JEOL JEM-3010 instrument, with an ultra-high resolution pole-piece (0.17 nm point resolution), equipped with a Gatan multi-scan CCD camera (Mod. 794) and an oxford EDS microanalysis detector. The powdered samples were dispersed in ethanol by sonication for approximately 5 min and deposited onto a holey carbon film grid.

Photoluminescence measurements were performed with a Fluorolog3-21 system (Horiba Jobin Yvon). A 450 W xenon arc lamp was used as a broadband excitation source and a double Czerny-Turner monochromator was used to select the excitation wavelength for photoluminescence excitation. All emission spectra were obtained using the same amount of powder, measured at room temperature and recorded under the same conditions.

The analysis of the emitted luminescence signal from the samples was performed by using a iHR320 single grating monochromator and a R5509 Hamamatsu photomultiplier tube detector. Time resolved characterization was recorded in multi channel single photon counting (MCSPC) mode by exciting the sample with a Nd-YAG laser NT 342/3/UVE/AW Ekspla, which can be tuned in the whole range 210–2300 nm. The pulse duration is about 6 ns at 10 Hz repetition rate.

The particle size was estimated from the X-ray line broadening of the (110) diffraction peak using the Scherrer formula [22].

$$D = 0.9\lambda/\beta \cos\ \theta, \tag{1}$$

where D is the particle size in nm, λ the radiation wavelength, θ the diffraction peak angle and β is the corrected line width at half-peak intensity. The correction for instrumental peak broadening was made using the Warren formula: $\beta=(b_{obs}^2-b^2)^{1/2}$, where b_{obs} is the line width at half-peak intensity related to $LaAlO_3$ powder and b is the line width of the (110) diffraction peak of the $LaAlO_3$.

4. Results and discussion

4.1. X-ray diffraction

The X-ray diffraction patterns of $LaAlO_3{:}Er^{3+}$ are shown in Fig. 1. According to XRD analysis (Fig. 1), the $LaAlO_3$ obtained at 800 °C crystallizes in a pure rhombohedral perovskite structure (JCPDS no. 01-082-0478) with space group R-3c (No.167), with unit cell dimensions a=5.37 Å and c=13.10 Å.

So all diffraction peaks in these XRD patterns could be attributed to the rhombohedral perovskite crystal structure of $LaAlO_3$ witch confirm that the doping concentration does not influence the crystalline phase formation.The particles size of $LaAlO_3$ powder calcined at 800 °C for 4 h calculated from the Scherrer formula is about 60 nm.

4.2. TEM and SEM analysis

Fig. 2a presents TEM micrographs of $LaAlO_3$:Er (5%) powders calcined at 800 °C, showing that the powders are composed by monocrystalline nanoparticles and exhibit the formation of aggregates among them. The nanoparticles have a polyhedral morphology with particle size about 60 nm, which agrees very well with the results given by the Scherrer formula.

Fig. 2b illustrates the high resolution TEM images (HRTEM), pointing out that the samples are perfectly crystalline, as can be seen by the uniform distribution of lattice planes.

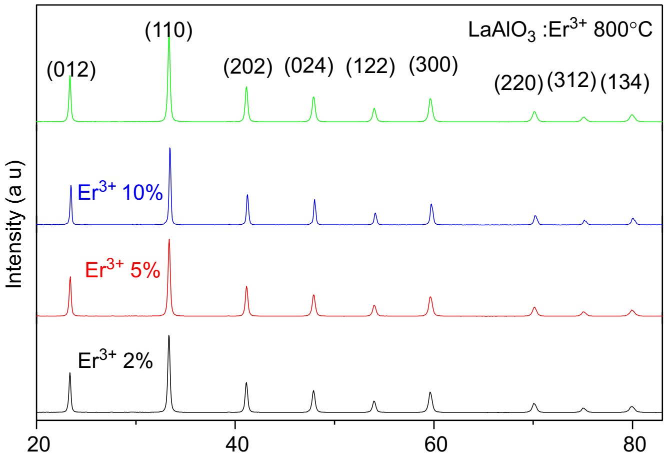

Fig. 1. X-ray diffraction patterns of $LaAlO_3{:}Er^{3+}$ observed and doping concentration variation.

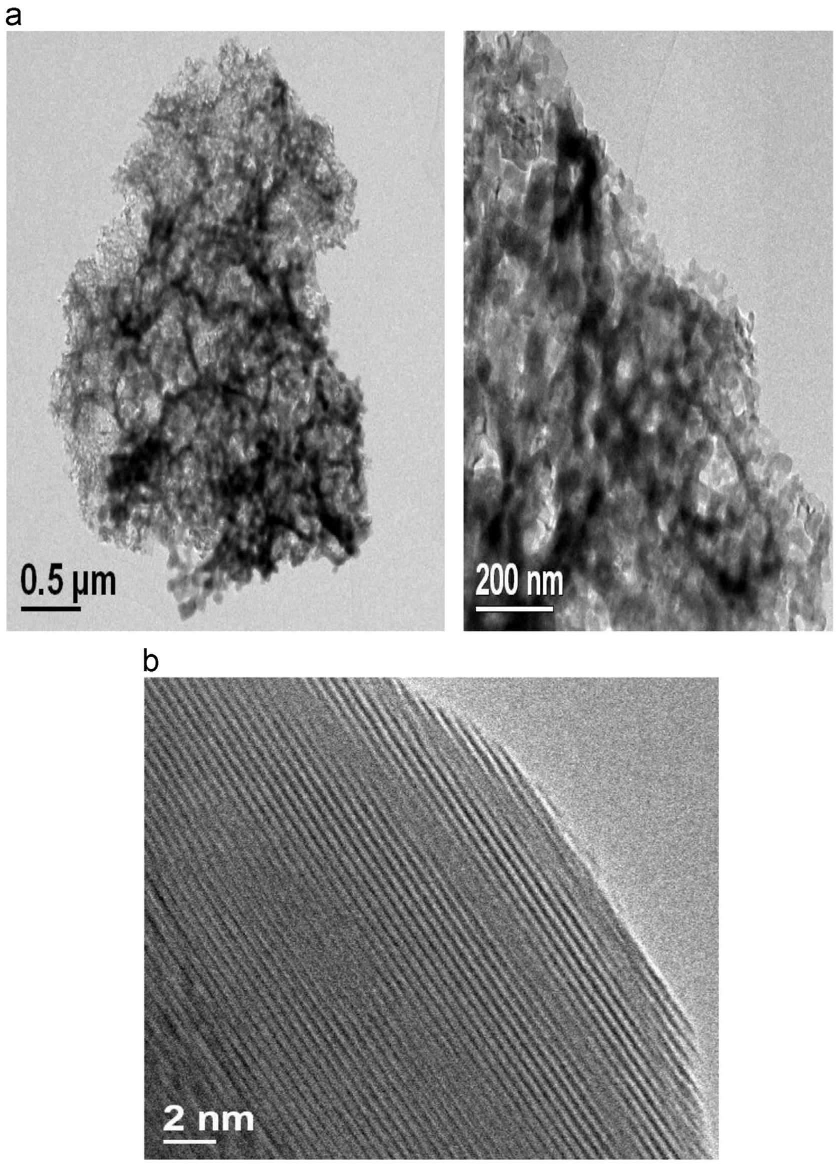

Fig. 2. (a) TEM micrograph and (b) HRTEM images and of $LaAlO_3$:Er (5%) obtained at 800 °C.

Fig. 3. shows SEM micrographs of $LaAlO_3$:Er (5%) annealed at 800 °C. The micrographs clearly indicate the porosity and agglomeration of polyhedral crystallites, which have no uniform shapes and sizes. This porosity can be assigned to the non-uniform distribution of temperature and mass flow in the combustion process. These porous powders are highly friable which facilitates easy grinding to obtain finer particles.

4.3. Photoluminescence studies

Optical properties of Er^{3+} doped $LaAlO_3$ was investigated first by Deren and all [23].

The excitation spectrum recorded at 1550 nm of 2% Er^{3+} doped $LaAlO_3$ is shown in Fig. 4.

The excitation spectrum consists of two intense peaks at 380 nm and 520 nm, which are assigned to ($^4I_{15/2} \rightarrow {}^4G_{11/2}$) and ($^2H_{11/2} \rightarrow {}^4I_{15/2}$), followed by weak shoulders at 365 nm, 406 nm, 448 nm, 486 nm, 540 nm and 648 nm.This peaks are attributed to ($^4I_{15/2} \rightarrow {}^4G_{9/2}$), ($^4I_{15/2} \rightarrow {}^4H_{9/2}$), ($^4I_{15/2} \rightarrow {}^4F_{5/2}$), ($^4I_{15/2} \rightarrow {}^4F_{7/2}$), ($^4S_{3/2} \rightarrow {}^4I_{15/2}$) and ($^4F_{9/2} \rightarrow {}^4I_{15/2}$) respectively.

The emission spectra under 378 nm excitation of Er^{3+} doped $LaAlO_3$ with different concentrations (2%, 5% and 10%) are shown in Fig. 5. The transition ($^4I_{13/2} \rightarrow {}^4I_{15/2}$) located at 1550 nm is the most intense.

The photoluminescence emission intensity increases with increasing Er^{3+} concentration (Table 1) from 2% to 5% and then decreases for higher concentrations, suggesting the occurrence of concentration quenching. The reason for concentration quenching is that the possibility of interaction between Er^{3+} ions also increases with increasing Er^{3+} concentration, allowing energy transfer and migration throughout the material until a defect can cause non radiative recombination. Therefore an excessive doping of rare earth ions

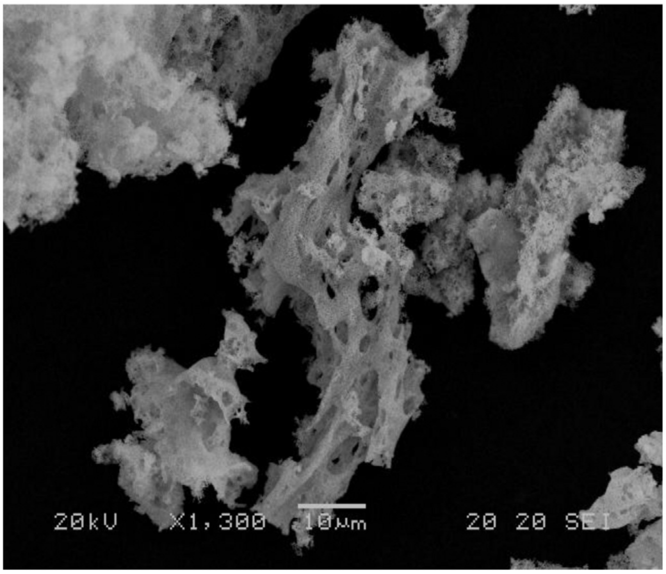

Fig. 3. SEM images of $LaAlO_3$: Er (5%) obtained at 800 °C.

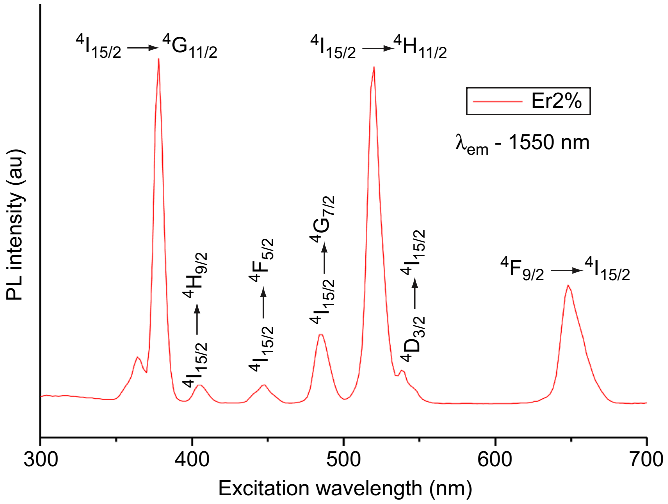

Fig. 4. Excitation spectrum of $LaAlO_3$:Er (2%).

should be avoided because it is detrimental for the phosphor efficiency.

Fig. 6 reports the decay time of ($^4I_{13/2} \rightarrow {}^4I_{15/2}$) at 1550 nm. These curves are not decreasing in a single exponential way, so they were fitted by a double exponential function. For this reason the values of lifetimes were obtained by an average calculation [24]:

$$\tau_{avg} \cong \frac{A_1\tau_1^2 + A_2\tau_2^2}{A_1\tau_1 + A_2\tau_2}$$

For the three concentration of Er^{3+} ions (2%,5%, 10%) we can see a decreasing of lifetime with increasing concentration: from 6.90 ms for the sample containing 2% of Er^{3+} ions to 5.87 ms for the sample containing 5% and 3.86 ms for the 10% concentration sample, in agreement with the hypothesis of concentration quenching [21].

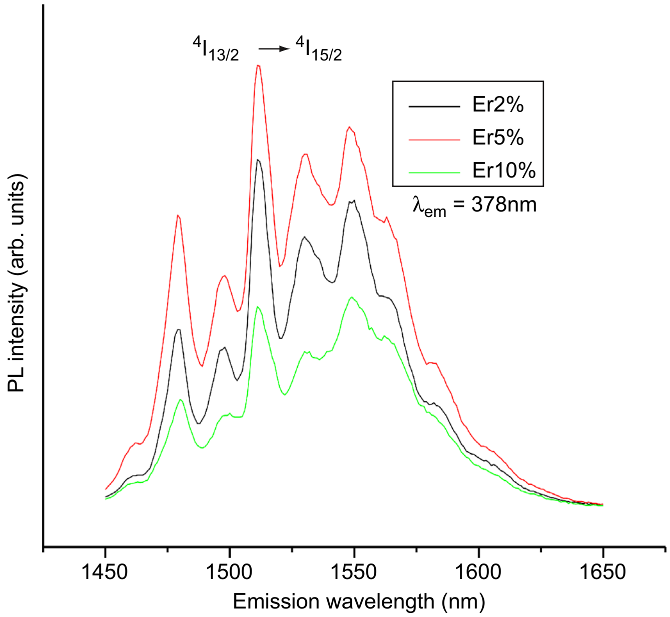

Fig. 5. Emission spectra of $LaAlO_3$:Er (2%,5%,10%) obtained at 800 °C.

Table 1
Dependence of the relative emission intensity of Er^{3+} on its doping concentration for Er-doped $LaAlO_3$.

Er concentration(%)	Normalized intensities of $^4I_{13/2} \rightarrow {}^4I_{15/2}$
2%	0.78
5%	1
10%	0.45

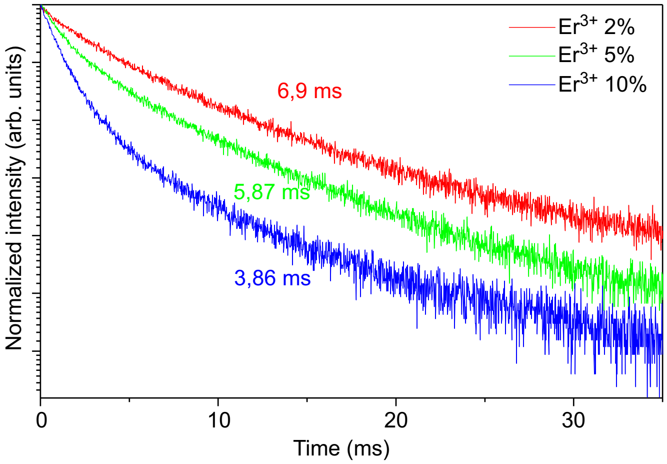

Fig. 6. Decay time of $LaAlO_3$:Er (2%, 5% and 10%).

5. Conclusion

A pure $LaAlO_3$ with a perovskite structure was obtained at 800 °C using a combustion method. The TEM image shows that we obtain a nanopowder with a particle size of about 60 nm. A strong luminescence at 1550 nm in the infrared (IR) region due to the ($^4I_{13/2} \rightarrow {}^4I_{15/2}$) transition has been observed in $LaAlO_3$:Er^{3+} phosphors. This intensity increases up to 5% of Er^{3+} ions in the sample, and then it decreases because of concentration quenching.

References

[1] C.J. Howard, B.J. Kennedy, B.C. Chakoumakos, Neutron powder diffraction study of rhombohedral rare-earth aluminates and the rhombohedral to cubic phase transition, Journal of Physics: Condensed Matter 12 (2000) 349.

[2] B. Jancar, D. Suvorov, M. Valant, G. Drazic, Characterization of $CaTiO_3$–$NdAlO_3$ dielectric ceramics, Journal of the European Ceramic Society 23 (2003) 1391.

[3] I. Zvereva, Y. Smirnov, V. Gusarov, V. Popova, J. Choisnet, Cation ordering and stability of the double perovskite slab—rocksalt layer P_2/RS intergrowth, Solid State Sciences 5 (2003) 343.

[4] M. Maczka, E. Mendoza-Mendoza, A.F. Fuentes, K. Lemanski, P. Deren, Low-temperature synthesis,luminescence and phonon properties of Er and/or Dy doped $LaAlO_3$ nanopowders, Journal of Solid State Chemistry 187 (2012) 249–257.

[5] J. Prado-Gonal, A.M. Arevalo-Lopez, E. Moran, Microwave-assisted synthesis: a fast and efficient route to produce $LaMO_3$ (M = Al, Cr, Mn, Fe, Co) perovskite materials, Materials Research Bulletin 46 (2011) 222–230.

[6] M. Kakihan, T. Okubo, Low temperature powder synthesis of $LaAlO_3$ through in situ polymerization route utilizing citric acid and ethylene glycol, Journal of Alloys and Compounds 266 (1998) 129.

[7] A.K. Adak, P. Pramanik, Synthesis and characterisation of lanthanum aluminate powder at relatively low temperature, Materials Letters 30 (1997) 269.

[8] M. Chroma, J. Pinkas, I. Pakutinskiene, A. Begankiene, A. Kareiva, Processing and characterization of sol–gel fabricated mixed metal aluminates, Ceramics International 31 (2005) 1123.

[9] S.N. Koc, F. Oksuzomer, E. Yasav, S. Akturk, M.A. Gurkaynak, Effect of sol–gel modifications on formation and morphology of nanocrystalline lanthanum aluminate, Materials Research Bulletin 41 (2006) 2291.

[10] A. Barrera, S. Fuentes, M. Viniegra, M. Avalos-Borja, N. Bogdan Chikova, J.C. Molina, Structural properties of Al_2O_3–La_2O_3 binary oxides prepared by sol–gel, Materials Research Bulletin 42 (2007) 640.

[11] Y. Xu, G. Huang, H. Long, Synthesis of lanthanum aluminate via the ethylenediaminetetraacetic acid gel route, Ceramics International 29 (2003) 837.

[12] D. Zhou, G. Huang, X. Chen, J. Xu, S. Gong, Synthesis of $LaAlO_3$ via ethylenediaminetetraacetic acid precursor, Materials Chemistry and Physics 84 (2004) 33.

[13] P.J. Deren, K. Lemanski, A. Gągor, A. Watras, M. Malecka, M. Zawadzki, Symmetry of $LaAlO_3$ nanocrystals as a function of crystallite size, Journal of Solid State Chemistry 183 (2010) 2095.

[14] R. Pazik, G.A. Seisenbaeva, R.J. Wiglusz, L. Kepinski, V.G. Kessler, Crystal structure and morphology evolution in the $LaXO_3$, X = Al, Ga, in nano-oxide series. Consequences for the synthesis of luminescent phosphors, Inorganic Chemistry 50 (2011) 2966.

[15] S. Ran, L. Gao, Synthesis of $LaAlO_3$ powder using triethanolamine, Ceramics International 34 (2008) 443.

[16] J.J. Kingsley, K.C. Patil, A novel combustion process for the synthesis of fine particle α-alumina and related oxide materials, Materials Letters 6 (1988) 427.

[17] M.D. Shaji Kumar, T.M. Srinivasan, P. Ramasamy, C. Subramanian, Synthesis of lanthanum aluminate by a citrate-combustion route, Materials Letters 25 (1995) 171.

[18] R. Nikifor, S.M. Glauco, Enhancement of luminescence efficiency of f–f transitions from Tb^{3+} due to energy transfer from Ce^{3+} in Al_2O_3 crystalline ceramic powders prepared by low temperature direct combustion synthesis, Chemical Physics Letters 400 (4–6) (2004) 553–557.

[19] N. Rakov, G.S. Maciel, W.B. Lozano, C.B. deAraujo, Investigation of Eu^{3+} luminescence intensification in Al_2O_3 powders codoped with Tb^{3+} and prepared by low-temperature direct combustion synthesis, Applied Physics Letters 88 (2006) 081908.

[20] A. Dhahri, K. Horchani-Naifer, A. Benedetti, F. Enrichi, M. Ferid., Combustion synthesis and photoluminescence of Eu^{3+} doped $LaAlO_3$ nanophosphors, Optical Materials 34 (2012) 1742–1746.

[21] A. Dhahri, K. Horchani-Naifer, A. Benedetti, F. Enrichi, M. Ferid, P. Riello, Combustion synthesis and photoluminescence of Tb^{3+} doped $LaAlO_3$ nanophosphors, Optical Materials 35 (2013) 1184–1188.

[22] P. Scherrer, Estimation of the size and internal structure of colloidal particles by means of röntgen, Cottin Nachrichten 2 (1918) 38.

[23] P.J. Deren, R. Mahiou, Spectroscopic characterisation of $LaAlO_3$ crystal doped with Er^{3+} ions, Optical Materials 29 (2007) 766.

[24] J.R. Lakowicz, Principle of Fluorescence Spectroscopy, 3rd ed., Kluwer Academic (Plenum Publisher), New York, 1999.